

Analysis of Cracked Plates and Shells, and its Application in Engineering

C. T. LIU (LIU CHUN-TU)
*Institute of Mechanics, Academia Sinica,
Beijing, 100080, PRC*

1. INTRODUCTION

The critical point in design and operation of pipes, vessels and aero- parts is dependent on the ability to Predict the rupture and failure of its most critical components. The analysis of numerous cases of failure revealed that in many incidences, failure occurred at stresses lower than design stresses. The origin of these failure has been found to be due to flaws which become critical as the stresses increase or which grow to a critical size during the cyclic operation of vessel. In order to predict such failure, it is essential in the design to consider the behavior of flaws under stress and the intensification of these stresses around the crack for prediction of crack initiation and subsequent propagation. Accurate evaluation of these stress intensity factors in plates, cylindrical and spherical shells is of great importance in the safety analysis of pressure vessels and aero-space parts.

The fracture problems of plates and shells is much more complicated comparing to in plane fracture, Strictly speaking, this is a three dimensional problem and different approximate theories for cracked plates and shells are actually different degrees of approximation to the accurate three dimensional analysis. Because of the difficulties, the numbers of papers about cracked plates and shells appeared in the literature is not great. Among those papers, most of them are dealt with the analysis for infinite plates and papers concerned the finite size of cracked plates are rare.

Nowadays, linear classical plate and shell theory is still the basis for analysing engineering problems, and the standard for design. It is badly needed to investigate the range within which classical plate and shell theory could give adequate results. More accurate calculation for stress intensity factors for finite cracked plates is also needed in engineering application.

This paper mainly summarize the research work carried out in our group during the past decade. Some of other author's investigation could not be included here, because of limited length of the paper. The characteristics of our research work are:

(1) Reissner's theory which account for transverse shear deformations is used to investigation cracked plate and shell, in order to avoid the defect of the classical theory and also make the analysis not too complicated.

(2) Analysis was started from study the stress strain field near the crack tip.

(3) The "local-global method" is used to analyse the cracked plates and shells, therefore more accurate calculation of stress intensity factors can be achieved.

2. THE DEFECTS OF CLASSICAL KIRCHHOFF'S PLATE THEORY IN FRACTURE MECHANICS

On the analysis of fracture problems for bending cracked plates, earlier studies were mainly based on Kirchhoff's theory that assume that a line vertical to the mid-plane remains unchanged in length and still vertical to the mid-plane after the deformation. It leads that deformation u, v, w of the plate can be expressed by one function $w(x, y)$ and the equilibrium equation is

$$D \nabla^2 \nabla^2 w = q \quad (2.1)$$

where D is bending stiffness.

$$D = Eh^3/12(1-\nu^2) \quad (2.2)$$

Three typical kinds of boundary conditions are as following

- 1) Fixed conditions: $w = \bar{w}, \quad w/n = \bar{\psi}_n$
- 2) Simple support conditions: $w = \bar{w}, \quad M_n = \bar{M}_n$
- 3) Free conditions: $M_n = \bar{M}_n, \quad \partial M_n / \partial s + Q_n = \bar{V}_n$

Along the free boundary, there should have three boundary conditions, but in Kirchhoff's plate theory, because of the governing equation is of fourth orders, only need two boundary conditions, so it is needed to introduce the effective shear force

$$V_n = \partial M_n / \partial s + Q_n \quad (2.3)$$

From the energy viewpoint, it can be proved that in Kirchhoff's theory M_n and Q_n is not independent. If displacement w get a variation δw , then the variational work

$$\delta A = \int_c (-M_{n,s} (\partial \delta w / \partial s) + Q_n \delta w) ds = -[M_{n,s} \delta w]_A + \int_c ((\partial M_n / \partial s) + Q_n) \delta w ds \quad (2.4)$$

so $V_n = \partial M_n / \partial s + Q_n$ is the general force corresponding to general displacement w . Therefore the conditions of free crack edge can not be satisfied exactly, if Kirchhoff's theory is employed to study fracture in plate.

Williams⁽¹⁾ expanded the displacement to a series of eigen-functions satisfying the boundary conditions in crack edge, and found the general expression near the crack tip for bending plate. Sin, G.S. and Paris, P.C.⁽²⁾ obtained the stress intensity factor for infinite plate by using the complex function method. The moments can be expressed by complex function:

$$\begin{aligned} M_x + M_y &= -4D(1+\nu)R_0 [\phi'(z)] \\ M_y - M_x + 2iM_{xy} &= zD(1-\nu) [\bar{z}\phi''(z) + \psi'(z)] \\ Q_x - iQ_y &= -4D\phi'''(z) \end{aligned} \quad (2.5)$$

and the complex stress intensity factor K can be defined as

$$K = K_I - iK_{II} \quad (2.6)$$

where K_I and K_{II} are the stress intensity factors for mode I and mode II respectively. The free crack edge boundary conditions may be written as (Fig 2.1)

$$M_n|_{y=0} = 0, \quad U_n|_{y=0} = 0 \quad (2.7)$$

If the displacement w is assumed as following:

$$w = \sum W_n(r, \theta) = \sum r^{3/2} F(r, \theta) \quad (2.8)$$

then

$$\begin{aligned} \sigma_r &= (K_I z / \sqrt{2\pi rh}) [(3+5\nu)/(7+\nu) \cos(\theta/2) - \cos(3\theta/2)] \\ \sigma_\theta &= (K_I z / \sqrt{2\pi rh}) [(5+3\nu)/(7+\nu) \cos(\theta/2) + \sin(3\theta/2)] \\ \tau_{r\theta} &= (K_I z / \sqrt{2\pi rh}) [-(1-\nu)/(7+\nu) \sin(\theta/2) + \sin(3\theta/2)] \\ \tau_{rz} &= 0(r^{-3/2}) \\ \tau_{\theta z} &= 0(r^{-3/2}) \end{aligned} \quad (2.9)$$

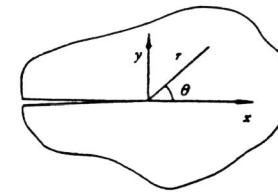


Fig.2.1

The singularity of shear stress is $r^{-3/2}$, which is different from the results obtained by three dimensional analysis. Since the shear deformation is neglected in classical theory, the shear force is not an independent one, therefore only two independent stress intensity factor can be obtained and stress intensity factor for mode III is not independent. Besides the angular variations of shear are not consistent to that of in-plane stresses. So the analysis of combination of tension and bending could not be carried out under classical theory. All of this are caused by the unsatisfaction of the free crack edge boundary conditions and the incorrect representation of the singularity near the crack tip.

For an infinite plate subjected to uniform bending moment M the stress intensity factor is

$$K_I = (12Z/h^3)M\sqrt{a}, \quad K_{II} = 0 \quad (2.10)$$

3. THE PLATE THEORY WHICH ACCOUNT FOR TRANSVERSE SHEAR DEFORMATIONS

(1) The Stress Singularity Near the Crack Tip.

Since 1960's the Reissner's plate theory was introduced into the analysis of bending cracked plate. The basic of the Reissner's plate theory is that any straight line vertical to the midplane remains a straight line and the length unchanged after deformation. This leads to the following expression:

$$\begin{aligned} u(x, y, z) &= -z\psi_x(x, y) \\ v(x, y, z) &= -z\psi_y(x, y) \\ w(x, y, z) &= w(x, y) \end{aligned} \quad (3.1)$$

where the ψ_x and ψ_y are rotations of a line in plane $x-z$ and $y-z$ respectively.

The equilibrium equation are

$$\begin{aligned}
 D \left(\frac{\partial^2 \psi_x}{\partial x^2} + \frac{1-\nu}{2} \frac{\partial^2 \psi_x}{\partial y^2} + \frac{1+\nu}{2} \frac{\partial^2 \psi_y}{\partial x \partial y} \right) + C \left(\frac{\partial w}{\partial x} - \psi_x \right) &= 0 \\
 D \left(\frac{\partial^2 \psi_y}{\partial x^2} + \frac{1-\nu}{2} \frac{\partial^2 \psi_y}{\partial x^2} + \frac{1+\nu}{2} \frac{\partial^2 \psi_x}{\partial x \partial y} \right) + C \left(\frac{\partial w}{\partial y} - \psi_y \right) &= 0 \quad (3.2) \\
 C \left(\frac{\partial^2 w}{\partial x^2} + \frac{\partial^2 w}{\partial y^2} - \frac{\partial \psi_x}{\partial x} - \frac{\partial \psi_y}{\partial y} \right) + P &= 0
 \end{aligned}$$

The analysis of the cracked plate based on Reissner's theory is very complex. Usually, the intergal transform method is used, and leads to solve an intergal equation. The typical work was done by Knoles and wang⁽¹³⁾. They first reached the result that all of the stresses have the same singularity ($r^{-1/2}$) near the crack tip and the angular distribution is the same as that of plane problems.

The stress field near the crack tip is

$$\begin{aligned}
 \sigma_x &= \frac{K_I(Z)}{\sqrt{2\pi r}} \cos \frac{\theta}{2} \left(1 - \sin \frac{\theta}{2} \sin \frac{3\theta}{2} \right) - \frac{K_{II}(Z)}{\sqrt{2\pi r}} \sin \frac{\theta}{2} \left(2 + \cos \frac{\theta}{2} \cos \frac{3\theta}{2} \right) + O(r^0) \\
 \sigma_y &= \frac{K_I(Z)}{\sqrt{2\pi r}} \cos \frac{\theta}{2} \left(1 + \sin \frac{\theta}{2} \sin \frac{3\theta}{2} \right) - \frac{K_{II}(Z)}{\sqrt{2\pi r}} \sin \frac{\theta}{2} \cos \frac{\theta}{2} \cos \frac{3\theta}{2} + O(r^0) \\
 \tau_{xy} &= \frac{K_I(Z)}{\sqrt{2\pi r}} \cos \frac{\theta}{2} \sin \frac{\theta}{2} \cos \frac{3\theta}{2} + \frac{K_{II}(Z)}{\sqrt{2\pi r}} \cos \frac{\theta}{2} \left(1 - \sin \frac{\theta}{2} \sin \frac{3\theta}{2} \right) + O(r^0) \\
 \tau_{xz} &= -(K_{III}(Z)/\sqrt{2\pi r}) \sin(\theta/2) + O(r^0) \\
 \tau_{yz} &= -(K_{III}(Z)/\sqrt{2\pi r}) \cos(\theta/2) + O(r^0)
 \end{aligned} \quad (3.3)$$

For an infinite plate subjected to uniform bending, the stress intensity factor can be expressed as

$$K(Z) = (12Z/h^3) \Phi(l) M \sqrt{a}$$

where the $\Phi(l)$ is the solution of the second kind of Fredholm's intergal equation.

It is an important progress to use Reissner's theory to analysis the cracked plate. an accurate stress strain field near the crack tip is obtained by Reissner's theory which accout for thansverse shear deformations which was neglected in Kirchoff's theory. This is supported by photo-elastic experiment done by smith, D.G. and smith, C.W.⁽¹⁷⁾. why the difference between the theory of kirchhoff's and Reissner's is so greatly. They are not only different in the distribution of the stresses near the crack tip, but also in the order of the singularity of the shear forces. Many literatures generally interpret them into the unsatisfaction of the free traction boundary condition. For more detail let us consider a simple example.

A rectangular plate subjected to uniform load on the surface, three of the edges are simple supported, and the other is free (Fig. 3.1 (a)), the shear

force Q in the line $x=a/2$ is shown in fig 3.1 (b).

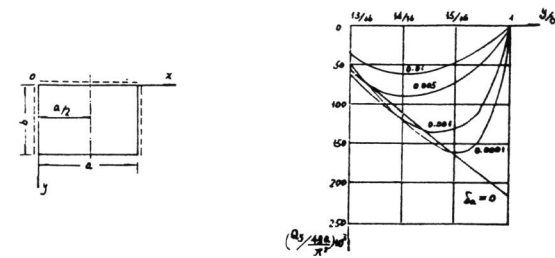


Fig 3.1 (a)

Fig 3.1 (b)

The shear deformation increase with the increase of dimensionless parameter $\delta_a = D/(c_s^2)$. If $\delta_a = 0$, corresponding to the neglect of the shear deformation. It can be seen from Fig.3.1 (b) that the value of Q_y are almost the same for all δ_a in the area far from the free edge, but for the area near the free edge the differences are great for different δ_a .

The smaller of δ_a , the more rapidly change in the value of Q_y , and also the smaller of the area effected by free edge. This means that in Reissner's theory, Q_y and M_{xy} is zero in the line $y=b$, but near the free edge in which line Q_y and M_{xy} is not small. So that there is a boundary layer Q_y and M_{xy} drop down rapidly.

Different from the Reissner's theory, an effective shear force V_y was introduced in Kirchoff's theory.

$$V_y = \partial M_{xy} / \partial x + Q_y \quad (3.4)$$

It change slowly near the free edge, and almost does not relate to the δ_a . The effective shear force conceal great change of Q_y , M_{xy} . So that Kirchoff's theory can not describe the real stress status near the free edge well, the Reissner's theory should be used.

Reissner's theory should be used to investigate the stress strain field near the crack tip, since the crack edge is also free edge.

Only the frist term of the stress strain field was given in[3,4]. The whole field near the crack tip was still unknown. In 1979, Muthy etc. found an displacement expansions for mode I in Reissner's plate. In 1980, Chun-tu Liu found an expansions for stress strain field near the crack tip for mode I, II and III, and expound the mechanical propriety near the crack tip in Reissner's plate. The expansions play the same role in plate as williams' expansion in cracked plane, and set up a sound foundation for mechanical analysis on cracked plate.

(2) The Solution for Stress Field near the Crack Tip.

(A) Perturbation method:

Let

$$\begin{aligned}
 \psi_r^{(\lambda)} &= r^\lambda (a_0^\lambda(\theta) + a_1^\lambda(\theta)r + a_2^\lambda(\theta)r^2 + \dots) \\
 \psi_\theta^{(\lambda)} &= r^\lambda (b_0^\lambda(\theta) + b_1^\lambda(\theta)r + b_2^\lambda(\theta)r^2 + \dots) \\
 w^{(\lambda)} &= r^\lambda (c_0^\lambda(\theta) + c_1^\lambda(\theta)r + c_2^\lambda(\theta)r^2 + \dots)
 \end{aligned} \quad (3.5)$$

substitute them into the equilibrium (3.2) and boundary conditions,

$$M_0 = M_{r,0} = Q_0 = 0 \quad (3.6)$$

the solutions were found in [13], perturbation.

(B) Displacement function Method ?

Based on Reissner's theory, the governing equations could be expressed in terms of three generalized displacements ψ_r, ψ_0 and w as formula (3.5).

Two displacement functions F and f also introduced, therefore

$$\phi_x = \partial F / \partial x + \partial f / \partial y \quad \phi_y = \partial F / \partial y - \partial f / \partial x \quad (3.7)$$

Substituting eq.(3.7) into (3.2). we have

$$\begin{aligned} \partial / \partial x [D \nabla^2 F + C(W-F)] + \partial / \partial y [(D/2)(1-\nu) \nabla^2 f - Cf] &= 0 \\ \partial / \partial y [D \nabla^2 F + C(W-F)] - \partial / \partial x [(D/2)(1-\nu) \nabla^2 f - Cf] &= 0 \end{aligned} \quad (3.8)$$

This the Cauchy-Riemann equation. from which it follows that

$$(D/2)(1-\nu) \nabla^2 f - Cf + i [D \nabla^2 F + C(W-F)] = C \phi(x+iy) \quad (3.9)$$

Separating the real part from the imaginary part in eq.(3.9).we have

$$\begin{aligned} \nabla^2 f - 4k^2 f &= 4k^2 \text{Re} \Phi & (a) \quad (3.10) \\ W = F - (D/C) \nabla^2 F + i m \Phi & & (b) \quad (3.10) \end{aligned}$$

where

$$4k^2 = 2C/D(1-\nu) = 10/h^2 \quad (3.11)$$

Substituting eqs (3.7) into eq. (3.2). we have

$$D \nabla^2 \nabla^2 F = p \quad (3.12)$$

For a cracked plate, the bending fracture problems are reduced to solve two equations, (3.10.a), (3.12) in terms of F and f with the Corresponding boundary conditions.

The function $\Phi(x+iy)$ could be expanded in series

$$\begin{aligned} \Phi(x+iy) &= \sum (\beta \mu + i \alpha \mu) \phi^n \\ &= \sum (\beta \mu + i \alpha \mu) \phi^n (\cos \mu \theta + i \sin \mu \theta) \end{aligned} \quad (3.13)$$

The solution of eqs (3.10.a), (3.12) could be expressed in the sum of a particular solution and the general solution of the corresponding homogeneous equations.

The particular solution could be chosen as follows

$$f_1 = -\text{Re} \Phi, \quad F_1 = 0 \quad (3.14)$$

The homogeneous equation corresponding to eq. (3.10.a) is

$$\nabla^2 f_0 - 4k^2 f_0 = 0 \quad (3.15)$$

When $p=0$, from eq. (3.12), we have

$$D \nabla^2 \nabla^2 F = 0 \quad (3.16)$$

Equation (3.16) is a biharmonic equation, we have

$$\begin{aligned} F(r, \theta) &= \sum r^{\lambda+1} F(\theta) \\ &= \sum r^{\lambda+1} [K_\lambda \cos(\lambda-1)\theta + L_\lambda \sin(\lambda-1)\theta + M_\lambda \cos(\lambda+1)\theta \\ &\quad + N_\lambda \sin(\lambda+1)\theta] \end{aligned} \quad (3.17)$$

Equation (3.15) is a Helmholtz's equation, function f could be expressed in modified Bessel's function. From the condition of finite strain energy, we should drop out the modified Bessel's function of the second kind and f could be expressed in modified Bessel's functions of the first kind $I_\lambda(2Kr)$ only.

For symmetric case

$$f_\lambda = \sin \lambda \theta I_\lambda(2kr) = \sin \lambda \theta \sum_{m=0,1,\dots} (k^2 r^{\lambda+2m} / m!) \phi(\lambda, m) \quad (3.18)$$

For anti-symmetric case

$$f_\lambda = \cos \lambda \theta I_\lambda(2kr) = \cos \lambda \theta \sum_{m=0,1,\dots} (k^2 r^{\lambda+2m} / m!) \phi(\lambda, m) \quad (3.19)$$

where

$$\begin{aligned} \phi(\lambda, m) &= (\lambda+1)(\lambda+2)\dots(\lambda+m) \quad (\text{for } m \geq 1) \\ \phi(\lambda, m) &= 1 \quad (\text{for } m=0) \end{aligned} \quad (3.20)$$

To determine the coefficients of expansion, it is convenient to express the general solution for eq.(3.15) in the following linear combination.

$$f_0 = \sum_{n=0,1,\dots} \sum_{m=0,1,\dots} (A_{\lambda-1+2n} f_{\lambda-1+2n} + B_{\lambda-1+2n} f_{\lambda-1+2n}^*) \quad (3.21)$$

Substituting eqs (3.17) and (3.21) into eqs (3.15), and (3.16), the linear equations whose unknowns are the coefficients of the expansions could be obtained. In order to satisfy these equations, we let

$$\lambda = \pm n/2 \quad n=0,1,2,\dots \quad (3.22)$$

With the condition of the finite strain energy, λ should be positive. By using the boundary conditions, the relations between coefficients in eigenfunction expansion could be found. with the known expression of F and f , the expression of ψ_r, ψ_0 and w as well as $M_r, M_0, M_{r,0}, Q_r, Q_0$, could be obtained.

This paper gives the general expansions of elastic stress-strain field at the crack tip in modes I, II and III for Reissner's plate. The expansions can serve as a basis for numerical methods for calculating stress intensity factors in plates, such as boundary collocation method, variational method, asymptotic method and higher order finite element method.

It has been pointed out in this paper that it is necessary to use basic equation of Reissner's theory (3.10) given in this paper for cracked plates.

(3) Numerical Examples.

Example 1. Infinite plate subjected to uniform bending moment. This problem was studied by Hartranft and Sih [2]. The stress intensity factor is

$$K_I(g) = (12Z/h^3) \phi(1) M \sqrt{\pi a} \quad (3.23)$$

The maximum value takes place at $z=h/2$.

$$K_I = (6M/h^2) \phi(1) \sqrt{\pi a} \quad (3.24)$$

In order to simulate infinite plate, the plate semilength L should be larger

than $20a$. The graph and result are shown in Fig (3.2) and (3.3), respectively.

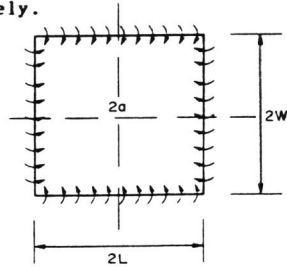


Fig.3.2 Cracked plate with uniform bending moment

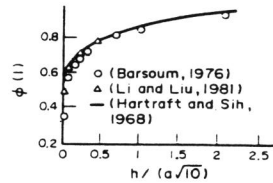


Fig.3.3 Comparison of authors solution with others

Example 2. Finite plate subjected to uniform bending moment. In order to investigate the variation of stress intensity factor of finite plate with different thickness and width, the stress intensity factor for $a/L=0.1, 0.2, 0.4$ and 0.5 are calculated. The results are shown in Fig (3.4). The finite size coefficients K_I / K_I are shown in Fig (3.5), where K_I denote K_I for infinite case.

Example 3. The effect of boundary conditions on the stress intensity factors. In order to compare the effect different boundary conditions on the stress intensity factors, the calculations for simple supported plate and free edge plate are carried out. The results are shown in Fig (3.6). In the calculation the bending moment is taken as 1 kg-cm/cm . and $h/a=1$.

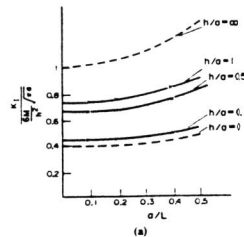


Fig.3.4 (a) Variation of stress intensity factors with plate width

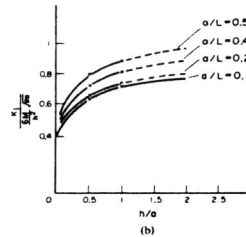


Fig.3.4 (b) Variation of stress intensity factors with plate thickness

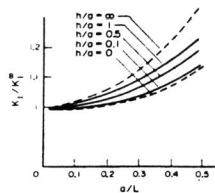


Fig 3.5 Finite size coefficient

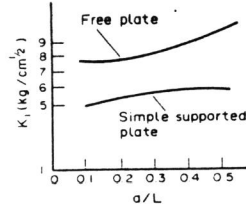


Fig 3.6 Effect of boundary conditions

Example 4. Cracked plate subjected to uniform twist moment. This is a mixed mode problems (Fig.3.7). For infinite case, this problem was studied by Delale [20] using an intergal transformation method. The dimensionless

stress intensity factors k_2 and k_3 are

$$\begin{aligned} k_2 &= K_{II}(h/2) / (6M/h^2) \sqrt{\pi a} \\ k_3 &= K_{III}(0) / (6M/h^2) \sqrt{\pi a} \end{aligned} \quad (3.26)$$

where $K_{II}(h/2)$, $K_{III}(0)$ are stress intensity factors for mode II and mode III, respectively. The maximum stress intensity factor for mode II takes place at plate surface, for mode III at the middle of the section. In order to simulate the infinite plate, we let $L=100a$, the solution compares favorably with that in ref. [20] (see Fig. 3.8).

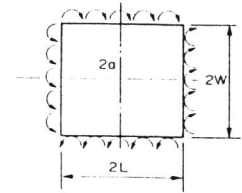


Fig.3.7 A cracked plate with uniform twist moment

For a finite size plate, the variation of the stress intensity factors with width and thickness is shown in Fig. 3.9.

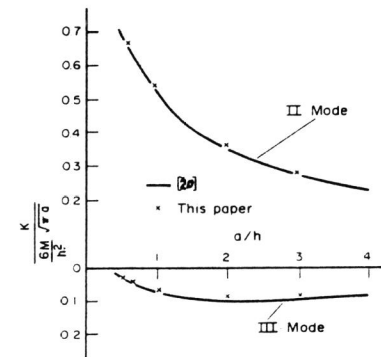


Fig.3.8 Comparison of authors solution with other (a/L -> 0)

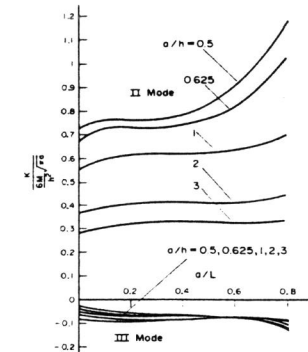


Fig.3.9 Variation of stress intensity factors with width and thickness

By using a higher order special element and hybrid technique, the stress intensity factors of infinite plate for mixed mode are calculated with higher accuracy both for mode II and mode III.

Both stress intensity factors K_{II} and K_{III} increase, with the increase of ratio a/L .

For mixed mode, the size of the special element should be taken $0.04-0.06 [a \cdot h]$ min.

For mixed mode, if the expansions of stress functions $M_x, M_y, M_{xy}, Q_x, Q_y$ in special element are taken as terms of $O(r^{3/2})$ the good results can be obtained.

(4) A path Independent Intergal in Reissner's plate.

Similar to J-integral in plane fracture problem, a J_n intergal in Reissner's plate was proposed [21], in which the authors employed virtual work theorem

to reach an integral independence to the path.

$$J_R = \int_c U dy + \int_c [-\bar{Q}_n (\partial W / \partial x) + \bar{M}_x (\partial \psi_x / \partial x) + \bar{M}_y (\partial \psi_y / \partial x)] ds \quad (3.27)$$

where U denotes the unit strain energy, M_x, M_y denote boundary moments, Qn denotes boundary shear.

The relation between J_R and stress intensity factors is

$$J_R = (h/8E) (K_I^2 + K_{II}^2) + (4h/15G) K_{III}^2 \quad (3.28)$$

J_R can be used in approximate analysis of stress intensity factor. It is also can be used as a parameter in elastic-plastic fracture analysis.

4. STUDY ON CRACK SPHERICAL SHELL FRACTURE PROBLEM

(1) The governing equations for cracked spherical shells

In the earlier literature the classical theory was used [18,19]. Even in present, many standards for engineering such as the standard for pressure vessel are still based on the classical theory for plates and shells. In recent years, Reissner's theory by using ten order differential equation was derived [25]. Since the problem is complicated, only the first term of the expansion was given [20,26,27]. In order to calculate stress intensity factors, the authors proposed an expansion of the stress-strain field at the crack tip including mode I, II and III, we also got some significant results in bulging factors.

The Stress-Strain Fields at Crack Tip in a Spherical Shell.

A spherical shell containing a through crack is shown in Fig. 4.1 with the crack tip at the origin of the coordinates. The shallow shell theory, taking into account of shear deformation, could be expressed as follows.

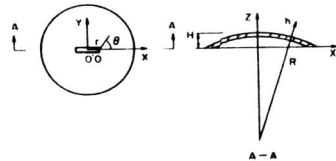


Fig.4.1 A cracked spherical shell

$$D \left(\frac{\partial^2 \psi_x}{\partial x^2} + \frac{1-\nu}{2} \frac{\partial^2 \psi_x}{\partial y^2} + \frac{1+\nu}{2} \frac{\partial^2 \psi_y}{\partial x \partial y} \right) + C \left(\frac{\partial W}{\partial x} - \psi_x \right) = 0 \quad (4.1)$$

$$D \left(\frac{1+\nu}{2} \frac{\partial^2 \psi_x}{\partial x \partial y} + \frac{1-\nu}{2} \frac{\partial^2 \psi_y}{\partial x^2} + \frac{\partial^2 \psi_y}{\partial y^2} \right) + C \left(\frac{\partial W}{\partial y} - \psi_y \right) = 0 \quad (4.2)$$

$$C \left(\frac{\partial^2 W}{\partial x^2} + \frac{\partial^2 W}{\partial y^2} - \frac{\partial \psi_x}{\partial x} - \frac{\partial \psi_y}{\partial y} \right) + k \nabla^2 \phi + q = 0$$

where k is the curvature, ϕ is the stress function

$$N_x = \partial^2 \phi / \partial y^2 \quad N_y = \partial^2 \phi / \partial x^2 \quad N_{xy} = -\partial^2 \phi / \partial x \partial y \quad (4.3)$$

the compatibility equation is

$$(1/B) \nabla^2 \nabla^2 \phi + k \nabla^2 W = 0 \quad (4.4)$$

where B is in plate stiffness.

Introducing displacement functions F and f, let

$$\psi_x = \partial F / \partial x + \partial f / \partial y \quad \psi_y = \partial F / \partial y - \partial f / \partial x \quad (4.5)$$

Substituting eq.(4.5) into eq. (4.1), we have eq.(3.8) again.

Similar as section 3, we have

$$D \nabla^2 F + C(W-F) = C \text{Im} \phi \quad (4.6)$$

$$(D/2)(1-\nu) \nabla^2 f - C f = C \text{Re} \phi \quad (4.7)$$

$$W = F - (D/C) \nabla^2 F + \text{Im} \phi$$

substituting eqs. (4.5), (4.7) into eq. (4.2), we have

$$D \nabla^2 \nabla^2 F - k \nabla^2 \phi = q \quad (4.8)$$

Substituting eq. (4.7) into eq.(4.4), we have

$$(1/B) \nabla^2 \nabla^2 \phi + k \nabla^2 F - k(D/C) \nabla^2 \nabla^2 F = 0 \quad (4.9)$$

The governing equations could be reduced to three eqs (4.6), (4.8) and (4.9) in terms of F, f and ϕ . The function f, which is similar to that in the bending plate case, is uncoupled. The functions F and ϕ should satisfy two fourth-order differential equations.

If $q=0$, from eq.(4.8), (4.9), we have

$$\nabla^2 \nabla^2 \nabla^2 F - (k^2 B/C) \nabla^2 \nabla^2 F + (k^2 B/D) \nabla^2 F = 0 \quad (4.10)$$

It can be proved that, function F in eq. (4.12) is the sum of following three functions F_0, F_1 and F_2 , which should satisfy the following equations respectively.

$$F = F_0 + F_1 + F_2 \quad (4.11)$$

$$\nabla^2 F_0 = 0 \quad (4.12)$$

$$\nabla^2 F_1 - 4\lambda_1^2 F_1 = 0 \quad (4.13)$$

$$\nabla^2 F_2 - 4\lambda_2^2 F_2 = 0 \quad (4.14)$$

where

$$4\lambda_1^2 = k^2 B/2C + \sqrt{k^4 B^2/4C^2 - k^2 B/D}$$

$$4\lambda_2^2 = k^2 B/2C - \sqrt{k^4 B^2/4C^2 - k^2 B/D}$$

If F is known, the ϕ could be obtained from eq. (4.6)

$$\phi = \phi_0 + (4D/k) (\lambda_1^2 F_1 + \lambda_2^2 F_2) \quad (4.15)$$

where ϕ_0 is an harmonic function, which should satisfy $\nabla^2 \phi_0 = 0$.

From eq.(4.6), function f could be found as

$$f = f_0 - \text{Re} \phi \quad (4.16)$$

f_0 should satisfy the following equation

$$\nabla^2 f_0 - 4\mu^2 f_0 = 0 \quad (4.17)$$

where $4\mu^2 = 2C/D(1-\nu)$ (4.18)

the boundary conditions are

$$M_\theta = M_{r,\theta} = Q_\theta = N_{r,\theta} = N_\theta = 0 \quad \text{when } \theta = \pm \pi \quad (4.19)$$

The analytic function Φ could be expanded in series

$$\Phi(x+iy) = \sum (\beta_n + ia_n) g^n = \sum (\beta_n + ia_n) r^n (\cos n\theta + i \sin n\theta) \quad (4.20)$$

Harmonic function F_0 could also be expanded in series

$$F_0 = \sum r^{\lambda+1} [K_{\lambda+1}^{(0)} \cos(\lambda+1)\theta + L_{\lambda+1}^{(0)} \sin(\lambda+1)\theta] \quad (4.21)$$

Functions f_0, F_1 and F_2 should satisfy eq.(4.17), (4.13), (4.14) respectively. These equations are Helmholtz's equations. Their solutions could be expressed in modified Bessel functions. With the condition of finite energy, we must drop out the modified Bessel functions of the second kind. The functions f_0, F_1 and F_2 could then be expressed in modified Bessel functions of the first kind only.

Similar to the bending cracked plate problem, substituting the expansions of f, F and ϕ into the boundary conditions eq. (4.19), the linear equations whose unknowns are the coefficients of the expansions could be established. From these equations, the relation between the coefficients in the eigenfunction expansion could be found. The generalized displacements and stress could be obtained after known the functions f, F and ϕ .

For the cracked spherical shells, a 10-th order differential equation could be reduced equivalently to a system of the uncoupled 2nd-order equations and a general solution (including Modes I, II, III) for stress-strain fields is found at crack tip which plays the same role as Williams' expansion for plane problems.

The crack-tip fields given in this paper extend numerical methods for plane problems, such as the energy method, the boundary allocation method and the high-order special element method, to the fracture analysis of shells, and provide a useful means for evaluation of stress intensity factors and even for mixed mode analysis

(2) Numerical Examples.

Mechanical behavior of finite-size spherical shell are investigated and it is shown that stress intensity factors increase with a/L under a bending load. The variation of stress intensity factor under different boundary conditions is also discussed.

When the shear stiffness is very large, there seems no difference between bulging factors obtained from Reissner's theory and classical theory. But as the shear stiffness becomes smaller, its effects become more and more significant and reach a maximum deviation of 46%. Generally, classical theories give a rather unsafe evaluation. For the convenience of engineering applications, we propose an approximate formula for bulging factor.

In order to obtain a satisfactory accuracy it is advisable to use an expression of displacement up to $r^{-7/2}$ and select the size of the special element as $0.1a$.

Fig. 4.1 shows a finite element mesh for a spherical shell containing a

central through crack, with $oxyz$ as global coordinates. A special element is used to represent the stress strain field at the crack tip, and the quadratic degenerate isoparametric thin shell element, which also takes into account transverse shear deformations, are used for ordinary element.

(A) Finite Size Spherical Shell subjected to Bending.

Infinite shell has been investigated by G.C.sih using an integral transform technique. However, as we know, the spherical surface cannot be geometrically extended to infinity, so the finite size ratio a/L is also a parameter that effects the value of the stress intensity factor. Fig.4.2 gives the stress intensity factors for different a/L values under a bending load. In the figure $\lambda = \sqrt{12(1-\nu^2)} a/\sqrt{Rh}$ is the curvature parameter. when $\lambda=0$, i.e. the case of flat plate, the numerical results approach the theoretical values obtained in [4] with an error less than 1% as $a/L \rightarrow 0$, and also agree very well with the results for finite plates obtained in [16]. When $\lambda > 0$, that is the case of shell, our results within the range of calculations, drop by a maximum of 30% compared with the theoretical values as a/L vanishes. This can be interpreted by the fact that for a given value of a/R , the shell goes deeper and deeper as a/L decreases, and the edge effect becomes more and more significant, and the assumptions for the shallow shell theory are no longer valid. This indicates that the results obtained in [22] are invalid for some ranges.

(B) Considering a spherical cap of $L/R = \pi/4$ under uniform pressure q , the stress intensity factors for different boundary conditions are given in Table 4.1 Compared with the stress intensity factors for free edge shells, the effect of simple support shell has a maximum decrease of 16%, and the effect of fixed support shell has a maximum decrease of 20%.

Table 4.1 Stress Intensity Factors Under Different Boundary Conditions ($\kappa=1$)

| λ | $K_I / (q_0 R / 2h) \sqrt{\pi a}$ | | |
|------------------|-----------------------------------|-------|-------|
| | 0.2 | 0.6 | 1.0 |
| Free edge | 1.222 | 1.593 | 1.800 |
| Simply Supported | 1.109 | 1.332 | 1.650 |
| Fixed | 1.065 | 1.271 | 1.579 |

(C) Bulging Factor.

Using Kirchhoff's classical thin shell theory, E.S.Folias (1965) obtained a formulation of stress intensity factor for pressurized spherical shell, which can be expressed as

$$K_I = M \sigma \sqrt{\pi a} \quad (4.22)$$

where $\sigma = qR/2h$ is the shell stress, q the uniform pressure, and M the bulging factor,

$$\text{in which } M = (1 + 0.59\lambda^2)^{1/2} \quad (4.23)$$

$$\lambda = \sqrt{12(1-\nu^2)} a/\sqrt{Rh} \quad (4.24)$$

The classical solution of bulging factor is only a function of λ . The application of Reissner's theory introduces a new mechanical parameter $\kappa = D/Ca^2$, which is the measure of transverse shear stiffness. Fig.4.2 expresses the distribution of bulging factor as a function of λ for various of κ . It follows from the result that for very small values of κ the bulging factor agrees well with the classical value (an error of about 1% for $\kappa=0.001$) and increases as κ increases. It has a maximum error of 46% within the range of our calculation.

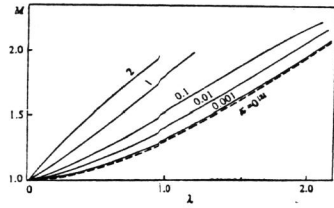


Fig. 4.2

Generally, in practical problems $\lambda < 2$, $\kappa < 2$, our calculation indicates that classical bulging factors are only valid for large a/h , otherwise it is preferable to use bulging factors on account of the shear stiffness.

Analysing the numerical results, we obtain an approximate formula for bulging factor

$$M(\lambda, \kappa) = M_1 (1 + 1.2 \kappa^{1/2} \lambda e^{-\lambda}) \quad \lambda < 2.2 \quad (4.25)$$

which involves an error of about 4%

5. AXIALLY CRACKED CYLINDRICAL SHELLS

The study of cracked cylindrical shell is of great importance in the safety analysis of engineering structures, such as pressure vessels, pipelines, etc. This problem was investigated first with the classical shallow thin shell theory [18,19] and then with Reissner's theory, both using integral equation approaches. Since the problem is complicated, only the first term of the stress expansion was given and stress intensity factors for infinite shells were evaluated. In [23] the quarter-point thick shell elements were applied to cylindrical shells with cracks. But these elements can only be used to approximate the stress fields in a region near the crack tip. In order to calculate stress intensity factors, it is necessary to use more general solution for stress-strain fields at the crack tip.

A perturbation method is used to solve the 10th-order differential equation of Reissner's shells. The analysis involves perturbation in a curvature parameter λ^2 ($\lambda^2 = [12(1-\nu^2)]^{1/2} a^2/Rh$). The perturbation solution, which takes transverse shear deformations into account, in a special element at the crack tip serves as shape functions. The 8-node thick shell elements are used for conventional element in the local-global analysis. Numerical result are obtained for symmetrical problems and the effect of finite size on stress intensity factor is discussed.

(1) The Governing Equations and Their Perturbation Solutions.

A cylindrical shell of radius R , thickness h , containing an axial through crack of length $2a$ is shown in Fig. 5.1, with the crack tip at the origin of the coordinates. The governing equations taking transverse shear deformations into account, are as follows:

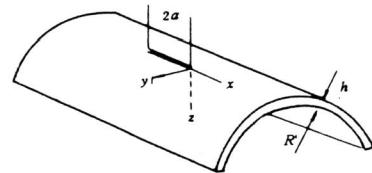


Fig. 5.1 Cylindrical shell with axial crack

$$D \left(\frac{\partial^2 \psi_x}{\partial x^2} + \frac{1-\nu}{2} \frac{\partial^2 \psi_x}{\partial y^2} + \frac{1+\nu}{2} \frac{\partial^2 \psi_y}{\partial x \partial y} \right) + C \left(\frac{\partial w}{\partial x} - \psi_x \right) = 0$$

$$D \left(\frac{\partial^2 \psi_y}{\partial y^2} + \frac{1-\nu}{2} \frac{\partial^2 \psi_y}{\partial x^2} + \frac{1+\nu}{2} \frac{\partial^2 \psi_x}{\partial x \partial y} \right) + C \left(\frac{\partial w}{\partial y} - \psi_y \right) = 0 \quad (5.2)$$

$$C \left(\nabla^2 w - \frac{\partial \phi_x}{\partial x} - \frac{\partial \phi_y}{\partial y} \right) + \frac{1}{R} \frac{\partial^2 \phi}{\partial x^2} + q = 0$$

$$(1/R) \nabla^2 \nabla^2 \phi + (1/R) (\partial^2 w / \partial x^2) = 0$$

Boundary conditions along the free crack edge are:

$$\theta = \pm \pi \quad M_y = M_x = Q_y = N_y = N_x = 0 \quad (5.2)$$

where ϕ is the stress function, $N_x = \partial^2 \phi / \partial y^2$, $N_y = \partial^2 \phi / \partial x^2$, $N = -\partial^2 \phi / \partial x \partial y$, w is deflection, and ψ_x and ψ_y are transverse shear deformations. B is tension compression stiffness; D is bending stiffness; C is shear stiffness. q is uniform pressure.

Introducing displacement functions F, f let

$$\psi_x = \partial F / \partial x + \partial f / \partial y \quad \psi_y = \partial F / \partial y - \partial f / \partial x \quad (5.3)$$

Substitute equation (5.3) into equation (5.1), after some mathematical manipulations we have:

$$\nabla^2 \nabla^2 \psi + \lambda^2 (\partial^2 w / \partial x^2) = 0$$

$$\nabla^2 \nabla^2 F - \lambda^2 (\partial^2 \psi / \partial x^2) = 0 \quad (5.4)$$

$$w = (1 - \kappa \nabla^2) F + \text{Im} \phi$$

$$\nabla^2 f - 4\mu^2 f = 4\mu^2 \text{Re} \phi$$

where $\psi = \phi / \sqrt{BD}$, $\lambda^2 = [12(1-\nu^2)]^{1/2} a^2/Rh$, $\kappa = D/Ca^2$, $4\mu = 1/(1-\nu)\kappa$, ϕ is an analytic function.

Expanding ψ, F, w in power series of λ^2 , we have

$$\psi = \sum_{n=0}^{\infty} \lambda^{2n} \psi_n \quad F = \sum_{n=0}^{\infty} \lambda^{2n} F_n \quad w = \sum_{n=0}^{\infty} \lambda^{2n} w_n$$

$$\phi = \sum_{n=0}^{\infty} \lambda^{2n} \phi_n \quad f = \sum_{n=0}^{\infty} \lambda^{2n} f_n \quad (5.5)$$

substituting equation (5.5) into equation (5.4), we get the perturbation equations:

$$\text{For } n=0$$

$$\nabla^2 \nabla^2 \psi_0 = 0$$

$$\nabla^2 \nabla^2 F_0 = 0$$

$$w_0 = (1 - \kappa \nabla^2) F_0 + \text{Im} \phi_0$$

$$\nabla^2 f_0 - 4\mu^2 f_0 = 4\mu^2 \text{Re} \phi_0 \quad (5.6)$$

For $n > 0$, we have,

$$\nabla^2 \nabla^2 \psi_n = -\partial^2 w_{n-1} / \partial x^2$$

$$\nabla^2 \nabla^2 F_n = \partial^2 \psi_{n-1} / \partial x^2$$

$$w_n = (1 - \kappa \nabla^2) F_n + \text{Im} \phi_n$$

$$\nabla^2 f_n - 4\mu^2 f_n = 4\mu^2 \text{Re} \phi_n \quad (5.7)$$

and details of solution for ψ_n, F_n, w_n and f_n , can be found in [17].

(2) The Calculation of Stress Intensity Factors

Fig. 5.2 shows a mesh adopted for an axially cracked cylindrical shell with OXYZ as the global coordinates. A special element is used to represent the stress-strain fields at the crack tip and the quadratic reduced intergration thick shell elements are used for conventional elements. Instead of Kirchhoff's assumption, we take the rotations as independent degrees of freedom in these elements and this is agreeable to that in high order shell theories, e.g. Reissner's theory.

Numerical results are given in the forms of stress intensity factors for two loading conditions, i.e. constant bending moment and uniform internal pressure. For constant bending moment M with maximum surface stress $\sigma_b = 6M/h$.

$$K_I = (K_{bb} + K_{bb}) \sigma_b \sqrt{\pi a} \tag{5.8}$$

and for uniform internal pressure q with membrane stress $\sigma_m = q R/h$.

$$K_I = (K_{mm} + K_{bb}) \sigma_m \sqrt{\pi a} \tag{5.9}$$

where K_{bb} , K_{mm} are stretching components of the stress intensity factors; and K_{bb} , K_{mm} are bending components of the stress intensity factors.

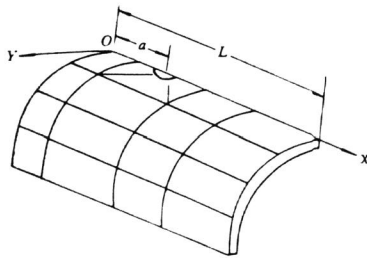


Fig.5.2 A mesh for cylindrical shell with axial crack

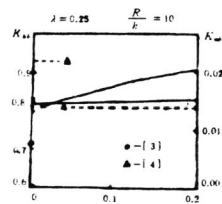


Fig.5.3 The variation of K_{bb} and K_{mm} with a/L

(A) Finite Size Cylindrical Shells under Constant Bending Moment.

A cylinder of length $2L$ is subjected to constant bending moment. The results are given in Fig.5.3 When $a/L=0.01$ the total intensity factor K_I compares very well with that obtained by [25] using quarter-point thick shell elements. The difference between them is about 14%.

(B) Cylinders Under Uniform Internal Pressure.

Numerical results are obtained for cylinders with the ratio $a/L=0.03$. Fig.5.4 and 5.5 show respectively the effect of shear stiffness on stretching and bending stress intensity factors K_{mm} and K_{bb} . It is noticed in the figures that when $\kappa \rightarrow 0$, K_{mm} approaches classical value but K_{bb} differs considerably from the thin shell theory result.

Combining the stretching and bending stress intensity factors we obtain the bulging factor:

$$M = K_{mm} + K_{bb} \tag{5.10}$$

which are given in Fig.5.4 shows that distribution of bulging factor as a

function of λ for various κ . We find that within the range of the calculation shear stiffness has a maximum effect of 33%. This error becomes larger while κ increases, since, at this time, the effect of shear stiffness is also included in it.

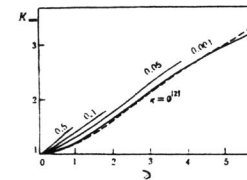


Fig.5.4 Stress intensity factors K_{mm}

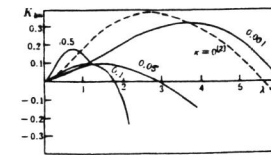


Fig.5.5 Stress intensity factors K_{bb}

Upon all of above, it can conclude following:

(a) For symmetric case (mode I), an asymptotic expression of displacements with expansion up to the term of $r^{7/2}$ is enough to obtain a good accuracy.

(b) Application of the stress-strain fields to a special crack tip element enable us to get more accurate evaluation of stress intensity factors than the quarter-point thick shell elements. The result is better than that of [24], which involves an error about 14%.

(c) Stress intensity factor increase with the ratio a/L .

(d) It follows the calculated results that the classical value of the stretching component of stress intensity factor seems to be the lower limit of the Reissner's theory.

(e) Within the range of the calculation, shear stiffness has a maximum effect of 33% on the bulging factor, and finite size has a maximum effect of about 12%.

6. CIRCUMFERENTIALLY CRACKED CYLINDRICAL SHELL

The stress strain fields at crack tip in a circumferentially cracked cylindrical shell (including Mode I, II, III,) are obtained by a perturbation technique, which provides a better function for evaluation of stress intensity factors. The asymptotic expressions of displacements are adopted up to the order of $O(r^{1/2})$ in the computation. The results show good agreement with the theoretical value.

It follows from the calculated results that the classical values of bulging factors, being the lower limit of those of Reissner's theory are only valid for very large ratio of a/h . Otherwise, the transverse shear effect should be taken into account.

A new approximate formula is given for bulging factors which includes the shear effect. With the range of our computation, it gives a better description of the bulging factor than the classical one.

Consider a cylindrical shell of radius R , thickness h , containing a circumferential crack of length $2a$, with the crack tip as the origin of the coordinates as shown in Fig.6.1. The governing equations can be expressed as H_u , (1981):

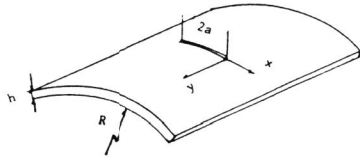


Fig.6.1 Cylindrical shell with a circumferential crack

$$\begin{aligned}
 D\left(\frac{\partial^2 \psi_x}{\partial x^2} + \frac{1-\nu}{2} \frac{\partial^2 \psi_x}{\partial y^2} + \frac{1+\nu}{2} \frac{\partial^2 \psi_y}{\partial x \partial y}\right) + C\left(\frac{\partial w}{\partial x} - \psi_x\right) &= 0 \\
 D\left(\frac{\partial^2 \psi_y}{\partial y^2} + \frac{1-\nu}{2} \frac{\partial^2 \psi_y}{\partial x^2} + \frac{1+\nu}{2} \frac{\partial^2 \psi_x}{\partial x \partial y}\right) + C\left(\frac{\partial w}{\partial y} - \psi_y\right) &= 0 \\
 C(\nabla^2 w - \partial \psi_x / \partial x - \partial \psi_y / \partial y) + (1/R)(\partial^2 \phi / \partial y^2) &= 0 \\
 (1/B)\nabla^4 \phi + (1/R)(\partial^2 w / \partial y^2) &= 0
 \end{aligned} \tag{6.1}$$

where ϕ is stress function, w is deflection, ψ_x and ψ_y are transverse shear deformations. B is stretching stiffness; D is bending stiffness, C is shear stiffness. Introducing displacement functions F, f , let

$$\psi_x = \partial F / \partial x + \partial f / \partial y, \quad \psi_y = \partial F / \partial y - \partial f / \partial x \tag{6.2}$$

substituting Eq.(6.2) into Eq.(6.1), after normalization of the coordinates with half crack length a and through some mathematical manipulations, we have:

$$\begin{aligned}
 \nabla^2 \nabla^2 \psi + \lambda^2 (\partial^2 w / \partial y^2) &= 0 \\
 \nabla^2 \nabla^2 F - \lambda^2 (\partial^2 \psi / \partial y^2) &= 0 \\
 w = (1 - \kappa \nabla^2) F + 1 \square \phi \\
 \nabla^2 \bar{f} - 4\mu^2 \bar{f} = 0 \quad f = \bar{f} - \text{Re } \phi
 \end{aligned} \tag{6.3}$$

where $\lambda^2 = [12(1-\nu^2)]^{1/2} a^2 / Rh$, $\kappa = D / Ca^2$, $4\mu^2 = 2 / (1-\nu) \kappa$, $\psi = \phi / \sqrt{BD}$, ϕ is analytic function. The boundary condition along the free crack edge are:

$$\theta = \pm \pi, \quad N_x = N_y = M_x = M_y = Q_x = Q_y = 0 \tag{6.4}$$

Expanding all the unknown function in power series of λ^2 , we have:

$$(F, f, \psi, w, \phi) = \sum_{k=0}^{\infty} \lambda^{2k} (F_k, f_k, \psi_k, w_k, \phi_k) \tag{6.5}$$

in which $\psi_k, F_k, \bar{f}_k, \phi_k$ are supposed to be the form as followings:

$$\begin{aligned}
 \psi_k &= \sum_{i,j} r^{i+1+2j} [A^{(k)} \cos(1+1+2i-2j)\theta + B_{i,j} \sin(1+1+2i-2j)\theta] \\
 F_k &= \sum_{i,j} r^{i+1+2j} [K^{(k)} \cos(1+1+2i-2j)\theta + B_{i,j} \sin(1+1+2i-2j)\theta] \\
 \phi_k &= \sum_{i,j} r^{i+1+2j} [\beta_{i,j} \cos(1-1+2i)\theta + i \alpha_{i,j} \sin(1-1+2i)\theta] \\
 f &= \sum_{i,j} r^{i+1+2j} [M_{i,j} \cos(1-1+2i-2n)\theta - N_{i,j} \sin(1-1+2i+2n)\theta]
 \end{aligned} \tag{6.6}$$

$$\begin{aligned}
 & \cdot \sum \frac{(-1)^n \mu^{2(m+n)} r^{1-1+2(1+m+n)}}{m! \phi(1-1+2i+2n, m) n! \phi(1+n-2+2i, n)}
 \end{aligned}$$

where $i = \sqrt{-1}$, $\phi(1, m) = \Gamma(1+m+1) / \Gamma(1+1)$, $\Gamma(1)$ is the Γ -function.

By properly choosing i 's and j 's both Eq. (6.3) and Eq. (6.4) can be satisfied in the sense that it only leaves term of $O(r^{2k-1/2})$

(A) Calculation of Stress Intensity Factors.

A finite element model is shown in Fig. 6.2 for a cylindrical shell containing a circumferential through crack. A special element is used to represent the stress strain fields at crack tip and the degenerate isoparametric thick shell elements (Zienkiewicz, 1971) are used as conventional elements. A good agreement is found between our result and the theoretical solution (Delale and Erdogan, 1979) when a/L approaches zero (with an error less than 2%).

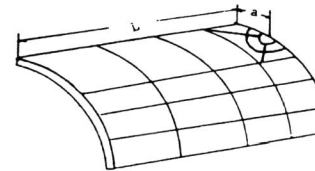


Fig.6.2

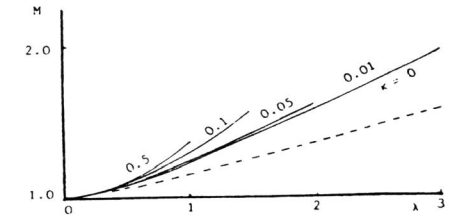


Fig.6.3 bulging factors

(B) Bulging Factors.

Folias (1967), using the classical thin shell theory obtained the bulging factor for a infinite long cylinder with circumferential crack, which depends only on the shell parameter. In our work using Reissner's theory, a new parameter $\kappa = D / Ca^2$ is introduced to the analyses to show the variation of bulging factors with shear stiffness. Numerical results are shown in Fig. 6.3, the distribution of bulging factors is a function of λ and κ . It is noticed that our results, although approaching to the classical solution for very small κ , show a maximum difference of about 30% when κ becomes larger.

The well known Folias formula which is currently used in engineering has the form of

$$M = (1 + 0.097 \lambda^2)^{1/2} \tag{6.7}$$

According to our analyses it gives rather an unsafe evaluation. Taking account the transverse shear stiffness, we propose a new formula of the following form:

$$M(\lambda, \kappa) = (1 + 0.097 \lambda^2)^{1/2} (1 + 0.25 \lambda \kappa^{1/10}) \tag{6.8}$$

which has an error less than 5% at a few point there it may reaches about 10%

Summary

In this paper so called "the local-global analysis" is used systematically for fracture analysis in cracked plates and shells. The general solutions of stress-strain fields at crack tip including mode I, mode II and mode III in Reissner's plates and shells were proposed. Similar to the Williams' expansion in plane fracture problem, they reveal the mechanical behavior near the crack tip and provide a better foundation for numerical fracture

analysis. The analytical method for the plane fracture problem, such as variation method, asymptotic method and finite element method, could be adopted for the plate and shell fracture analysis.

Based on the stress-strain fields, several kinds of high-order special elements were proposed to substitute the dense mesh near the crack tip. Meanwhile, since more accurate displacement modes are used, the accuracy of calculation could be improved. For some complex problem, such as in the case of mixed mode problems, more terms of the expansions is needed.

For plate and shell fracture analysis, the Reissner's theory was used to avoid the defect of classical theory. There is obvious difference between the results calculated by using different theories.

It have been found that the classical values of bulging factors are the low limits of those from Reissner's theory, and are only valid for very thin shells. In other case the transverse shear effect should be taken into account. New formulae for bulging factors is proposed in [14,15,17].

Since fracture mechanics is used in engineering, it have achieved greatly, but even in the area of the plate and shell fracture there are many problems reminded unsolved, such as the mechanical behavior of elastic-plastic plate containing a crack, crack closing in a plate, and variation of the fracture parameter with the coordinate along the thick direction. It is also urged that to find more accurate and less expensive method for engineering practise.

REFERENCES

- M. L. Williams, *J. appl. Mech.* 28, 78-82 (1961).
G. C. Sih and P. C. Paris, *J. Appl. Mech.* 29, 306-310 (1962).
J. K. Knowles and N. M. Wang, *J. Math. Phys.* 39, 223--236 (1960).
R. J. Hartranft and G. C. Sih *Math. Phys.* 47 (1968).
G. C. Sih, *Int. Fract. Mech.*, 7, 39-67 (1971).
Reissner, E. *Quarterly of Appl. Math.*, 5, 55-68 (1947).
Smith, D. G. and Smith, C. W. *Int. J. Fract. Mech.*, 63, 305-318 (1970).
Wilson, W. K. and Thompson, D. G., *Eng. Fract. Mech.* 3, 2 (1971).
Barsoum, R. S., *Int. J. for Num. Mech. in Eng.*, 10, 551-564, (1976).
Zienkiewicz, O, C, *The finite method in engineering science*, MCGRAW-HILL, London.
Yagawa, G., *Int. J. Num Mech* , 14, 5 (1979).
Jalees Ahmad and Francis-T. C. 100, *Eng , Fract. Mech.* 11.4, (1979)
Liu Chun-tu, *Acta Mechnica Solida Sinica*, 3, 41-448, (1983).
Liu Chun-tu, Wu Xijia, and Li Yingzhi, *Scienta Sinica (section A)*, Vol. XXX, No. 9 (1987).
Liu Chun-tu, Wu Xijia, *Acta Mechnica Sinica*, Vol. 19, No.2 (1983).
Li Yingzhi, Liu chuntu, *Acta Mechnica Sinica*, Vol. 14, No. 4, (1983).
Liu Chuntu, WQu Xijia, *Acta Mechnica Sinica*, 1987, No. 3.
Folias, E. S., *Int. J. Fract.*, 1 (1965), 20-46.
Erdogan, F. & Kibler, J., *INT. J. Fract.*, 1 (1969), 229-237.
Delale, F. & Erdogan, F., *Int. Solid struct.*, 15 (1979), 365.
Liu Chun-tu, Hu haichang, *J. Taiyuan Heavy Mech. Inst.*, 2, (1985).
Sih, G. C. and Hagendorf, H. C., *Thin Shell Structure*, 1974, 365-375.
Krenk, S., *Int. J. Fract. Mech.* 14 (1978), 123.
Barsoum, R. S. and Loomis, R. S. and Loomis, R. W., *Int. J. Fract. Mech.*, 15 (1979), 259.
P. M. Nahdi, *Q. Appl. Mech.* 54, 369-380, (1957).
G. C. Sih and H. C. Hagendorf, *Mechanics of Fracture*, (Edited by G. C. Sih) Vol. 3 (1973).
F. Delale, *Int. J. Engng. Sci.*, 20, 1325-1347 (1982).